2-Aminopurine-Modified DNA Homopolymers for Robust and Sensitive Detection of Mercury and Silver

Wenhu Zhou[1,2], Jinsong Ding[1] and Juewen Liu[1,2]*

[1]. School of Pharmaceutical Sciences, Central South University, Changsha, Hunan, China, 410013.

[2]. Department of Chemistry, Waterloo Institute for Nanotechnology, University of Waterloo, Waterloo, Ontario, Canada, N2L 3G1.

*Email: liujw@uwaterloo.ca

Abstract

Heavy metal detection is a key topic in analytical chemistry. DNA-based metal recognition has advanced significantly producing many specific metal ligands, such as thymine for Hg^{2+} and cytosine for Ag^{+}. For practical applications, however, robust sensors that can work in a diverse range of salt concentrations need to be developed, while most current sensing strategies cannot meet this requirement. In this work, 2-aminopurine (2AP) is used as a fluorescence label embedded in the middle of four 10-mer DNA homopolymers. 2AP can be quenched up to 98% in these DNA without an external quencher. The interaction between 2AP and all common metal ions is studied systematically for both free 2AP base and 2AP embedded DNA homopolymers. With such low background, Hg^{2+} induces up to 14-fold signal enhancement for the poly-T DNA, and Ag^{+} enhances up to 10-fold for the poly-C DNA. A detection limit of 3 nM is achieved for both metals. With these four probes, silver and mercury can be readily discriminated from the rest. A comparison with other signaling methods was made using fluorescence resonance energy transfer, graphene oxide, and SYBR Green I staining, respectively, confirming the robustness of the 2AP label. Detection of Hg^{2+} in Lake Huron water was also achieved with a similar sensitivity. This work has provided a comprehensive fundamental understanding of using 2AP as a label for metal detection, and has achieved the highest fluorescence enhancement for non-protein targets.

Keywords: biosensors; aptamers; DNA; metal ions; fluorescence

1. Introduction

Mercury and silver are toxic heavy metals but they are useful for a diverse range of applications. Their bio-accumulative property poses a severe threat to human health (Clarkson et al. 2003; Ratte 1999). To manage their contamination problem, efforts have been made to develop sensors for their on-site and real-time detection (Kim et al. 2012; Nolan and Lippard 2008), including using monoclonal antibodies (Zhou et al. 2011). These two metals are discussed together here since they are both strongly thiophilic with a similar redox potential, making it a challenge to accurately distinguish them sometimes.

Over the past two decades, DNA has become quite popular for metal sensing (Li et al. 2010; Liu et al. 2009; Wang et al. 2009a; Zhan et al. 2016; Zhang et al. 2011), which is attributable to its stability, programmability, versatile metal coordination chemistry, and ease of modification. For silver and mercury, in particular, a number of DNA-based sensing strategies have been developed. For example, DNAzymes (i.e. catalytic DNA) were isolated using Hg^{2+} and Ag^{+} as specific metal cofactors for RNA cleavage (Hollenstein et al. 2008; Saran and Liu 2016). In addition, their strong thiophilicity has allowed cleavage of phosphorothioate (PS)-modified RNA for biosensor design (Huang and Liu 2014; Huang et al. 2015). The fluorescence of some DNA-stabilized metal nanoclusters can be quenched or shifted by Hg^{2+} and Ag^{+} (Lee et al. 2015; Morishita et al. 2013; Shiang et al. 2012).

The most popular sensing methods have relied on the specific formation of thymine-Hg^{2+}-thymine (Ono and Togashi 2004), and cytosine-Ag^{+}-cytosine base pairs (Ono et al. 2008). In both cases, the target metal converts T-T and C-C mismatches to stable base pairs (Li et al. 2008; Li et al. 2009b; Miyake et al. 2006; Ono et al. 2011; Tanaka et al. 2007). These are

attractive due to reversible metal binding and simplicity. A careful examination of related literature has however identified a few limitations, and here we focus our discussion on fluorescence-based sensors. Some signaling methods rely on end-to-end distance change, where fluorescence resonance energy transfer (FRET) is often used (Ono et al. 2008; Ono and Togashi 2004). This method is highly susceptible to variations in ionic strength, since the end-to-end distance can also be changed by non-specific salt-induced DNA condensation (Kiy et al. 2012). Second, DNA staining dyes such as SYBR Green I were used (Lin and Tseng 2009; Wang and Liu 2008). While simple and cost-effective, it is prone to artifacts (e.g. dye adsorption by other nucleic acids or surfaces), and the dye/DNA binding is also dependent on salt concentration. The third strategy relies on the structure-switching mechanism (Nutiu and Li 2003; Wang et al. 2008), which is difficult to achieve reversible sensing and is likely also sensitive to ionic strength. For practical applications, robust and reversible sensors still need to be designed.

2-Aminopurine (2AP) is a fluorescent adenine analog that has been extensively used for probing nucleic acids (Hall 2009; Jones and Neely 2015). When a 2AP is introduced into a DNA structure, its fluorescence yield decreases significantly because of stacking with adjacent bases. While 2AP is an excellent probe to study DNA folding, its analytical applications have not been extensively explored (Katilius et al. 2006; Li et al. 2009a; Martí et al. 2006; Soulière et al. 2011). A major advantage of 2AP is strong fluorescence quenching (can reach >98%) without an external quencher (just quenched by adjacent nucleobases) (Jones and Neely 2015). Given these merits, little is known about its interaction with heavy metals. In this work, we designed four DNA homopolymers probes, each with an embedded 2AP. When used together to form a sensor array, they can distinguish Ag^{+} and Hg^{2+} from the rest with up to 14-fold fluorescence enhancement.

2. Materials and Methods

2.1. Chemicals. All the DNA samples were obtained from Integrated DNA Technologies (Coralville, IA). The metal salts and the free 2AP base were from Sigma-Aldrich. All the buffers were from Mandel Scientific Inc. (Guelph, Ontario, Canada). Milli-Q water was used to prepare all the buffers and solutions.

2.2. Fluorescence spectroscopy. Free 2AP base or 2AP-modified DNAs (1 μM) were dissolved in buffer A (10 mM MOPS, pH 7.0, adjusted by adding HNO_3 and NaOH). The fluorescence spectra were measured using a fluorometer (FluoroMax-4, Horiba Scientific) with 310 nm excitation and the emission at 370 nm was used for quantification. To measure the effect of metal ions, free 2AP base or 2AP modified DNAs (0.1 μM) were dissolved in buffer A, and their initial fluorescence spectra were recorded as described above. The fluorescence was measured immediately after adding a small volume of metal salt solution.

2.3. Hg^{2+}/Ag^{+} detection. The 2AP-modified DNA sensors (0.1 μM) were dissolved in buffer A. The 2AP fluorescence at 370 nm was monitored immediately after each addition of Hg^{2+}, Ag^{+} or other metal ions. To test reversibility, the Hg^{2+} sensor was added with 400 nM Hg^{2+}. After continuously monitoring for 5 min, 800 nM NaI was added, followed by 5 min fluorescence reading. The process was repeated for four times. To test the sensor performance in Lake Huron water, 1 μL T10-2AP DNA (100 μM) and 10 μL MOPS (1 M, pH 7.0) were added to 1 mL Lake Huron water. Then, 200 μL of the sample was titrated with Hg^{2+}, and the 2AP emission was recorded.

2.4. Other Hg^{2+} sensors. To graphene oxide (GO) based probe, 6-carboxyfluorescein labeled Hg^{2+}-binding DNA (4 μM, the sequence shown in Figure 4B) was mixed with nano-sized GO

(200 μg/mL) in buffer B (2 mM Mg^{2+}, 50 mM NaCl, 10 mM HEPES, pH 7.6). After 30 min incubation, the sensor was washed after centrifugation at 15,000 rpm for 30 min, and then re-dispersed in buffer A (with 100 nM adsorbed DNA). Then, the sensor was added with 400 nM Hg^{2+} in absence or presence of 100 mM $NaNO_3$. The fluorescence kinetic was monitored by a SpectraMax M3 microplate reader (Ex = 480 nm; Em = 526 nm) for 1 h. For SYBR Green I (SG) based probe, the Hg^{2+}-binding DNA (100 nM) and SG (250 nM) were diluted in buffer A. In absence or presence of 100 mM $NaNO_3$, 400 nM Hg^{2+} was added, and the fluorescence change was measured by a FluoroMax-4 fluorometer (Ex = 480 nm; Em = 515-570 nm). The peak intensity at 525 was used for quantification.

3. Results and Discussion

3.1. Mechanism of 2AP signaling. The structures of adenine and 2AP are shown in Figure 1A. They differ only by the position of the exocyclic amine group. Free 2AP emits strongly at 370 nm with a quantum yield of 0.68 (Jones and Neely 2015), while adenine is essentially non-fluorescent. Interestingly, the 2AP fluorescence is strongly quenched after incorporation into an oligonucleotide, attributable to stacking with neighboring nucleobases facilitating electron transfer (Kelley and Barton 1999), and collision by other bases (Rachofsky et al. 2001).

We first systematically studied the interaction between 2AP and heavy metals. Four probes were designed here, each inserting a 2AP in the middle of a 10-mer DNA homopolymer (Figure 1B). The fluorescence spectra of the free 2AP base and these four probes at the same concentration are shown in Figure 1C. In a polypyrimidine (C and T), the 2AP emitted 4 to 7-fold less compared to that in a polypurine (A and G). Their quenching efficiencies are shown in

Figure 1D. The T10-2AP DNA reached the highest quenching of ~98%, with the quenching order being T≅C>A≅G. Larsen and coworkers used dinucleotides and reported a 2AP quenching order of G>T≅A>C (Larsen et al. 2004). On the other hand, Ross *et al* showed that 2AP is quenched more by flanking thymines than by adenines, which is consistent with our results (Rachofsky et al. 2001).

Such a strong quenching is very impressive considering the lack of external quenchers. For example, a 98% quenching compares favorably to that achieved by molecular beacons with a nearby dark quencher (Tyagi and Kramer 1996; Wang et al. 2009b). In our system, quenching is achieved solely by DNA bases. This quenching is also different from the typical fluorophore quenching by DNA. In those cases, guanine is the strongest quencher but it quenches nearby fluorophores by only ~2-fold (Nazarenko et al. 2002). Such a strong 2AP quenching gives a large room for potential signal enhancement and thus high sensitivity.

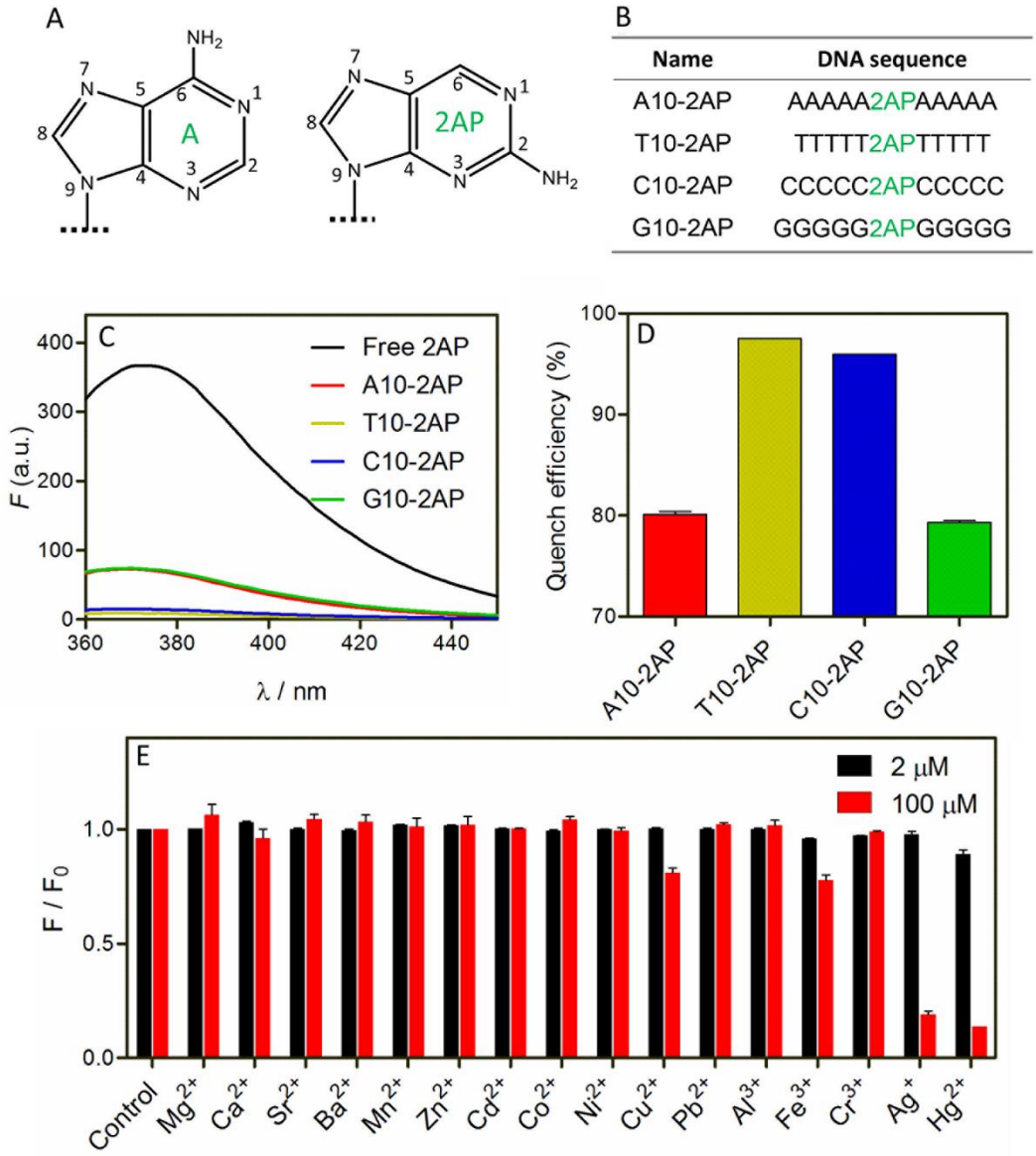

Figure 1. (A) The structures of adenine and 2AP. (B) The names and sequences of the DNAs used in this study. 2AP is inserted in the middle of each sequence. (C) Fluorescence spectra of the free 2AP base, and the four DNAs (1 μM each). (D) Quench efficiency of 2AP in the different DNA sequences. (E) Quench efficiency of the free 2AP base by metal ions.

3.2. Quenching of free 2AP by metal ions. Before testing our DNA probes, we mixed various metal ions with the free 2AP base. With 2 μM metals (Figure 1E, black bars), only Hg^{2+} caused ~10% quenching. This suggests a relatively low binding affinity between the metal ions and free 2AP. With 100 μM metals (2 mM for Mg^{2+} and Ca^{2+}), Hg^{2+} still yielded the strongest quenching of 86% (Figure 1E, red bars), followed by Ag^{+} (~80%) and Cu^{2+} and Fe^{3+} (~20 %). Most other metals again failed to quench. It is interesting to note that the ability to quench the 2AP emission correlates well with the thiophilicity of the metals, suggesting specific binding. Overall, non-specific quenching of 2AP by the metals is quite low. At the same time, no fluorescence enhancement was observed.

3.3. Emission enhancement by Hg^{2+} and Ag^{+}. We next titrated various metal ions to each of the four DNA probes. Since each probe has a different initial fluorescence (Figure 1C), we plotted the relative fluorescence change (F/F_0) after adding metal. Addition of 2 μM metals to the A10-2AP DNA (0.1 μM) caused <10% fluctuation in most cases (Figure 2A). The most significant quenching occurred with Ag^{+} (~20%) and Hg^{2+} (~30%). Since the free 2AP base was quenched much less (Figure 1E), DNA binding to these metals also contributes to the quenching. The G10-2AP DNA is more susceptible to metal-induced quenching (Figure 2B). In these two DNAs, metal binding might induce electron transfer to paramagnetic metals (e.g. Cu^{2+}) or enhance stacking of 2AP with its neighboring bases, resulting in fluorescence quenching.

We next tested the T10-2AP DNA (Figure 2C). Interestingly, Hg^{2+} enhanced its fluorescence by >7-fold, while most other metals failed to trigger a fluorescence change. Its high specificity for Hg^{2+} can be explained by the formation of T-Hg^{2+}-T base pairs, reducing stacking between the 2AP and its adjacent thymines. The strong initial quenching of 2AP by thymine (~98%) also gives a large room for signal enhancement.

Finally for the C10-2AP DNA, Ag^+ produced the strongest fluorescence enhancement followed by Hg^{2+} (Figure 2D). The effect of Ag^+ can be explained by formation of the C-Ag^+-C complex (Ono et al. 2008). It was previously reported that Ag^+ can be chelated by pyrimidine bases in general (Urata et al. 2011), but we did not see its signal in the T10-2AP DNA. On the other hand, Hg^{2+} induced a strong signal in the poly-C DNA, suggesting that cytosine is also a ligand for Hg^{2+}. Note that for all these experiments, we used only 0.1 μM DNA. Metal ions at 2 μM were in large excess. The C10-2AP DNA has much higher selectivity for Ag^+ over Hg^{2+} at lower metal concentrations (vide infra).

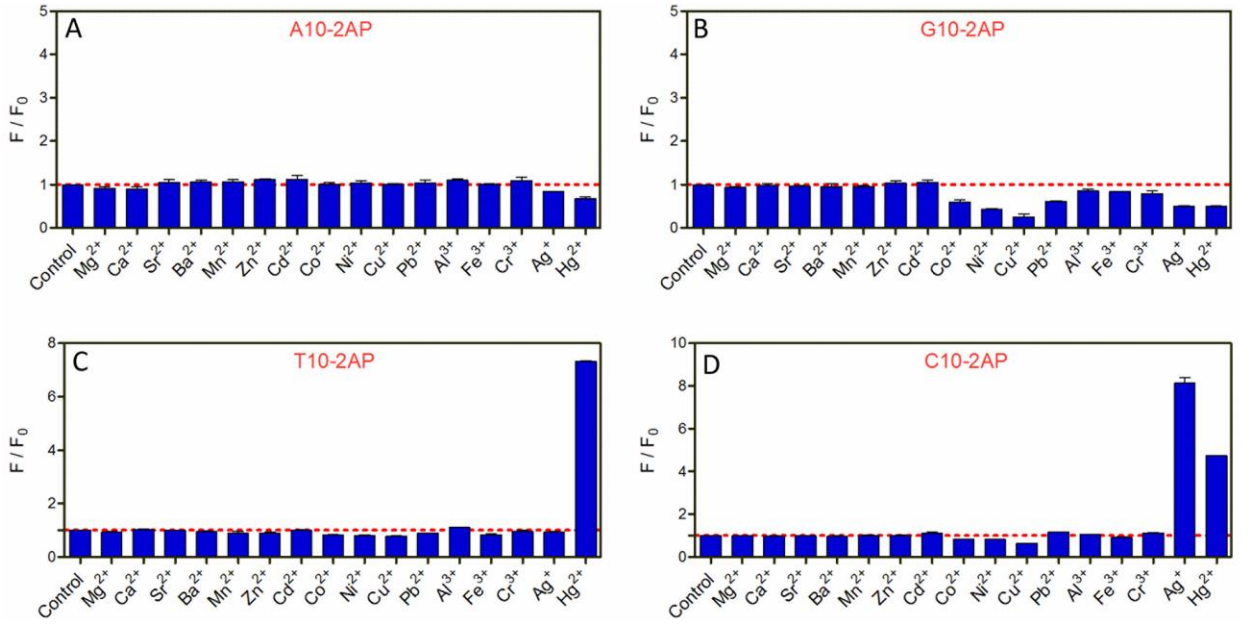

Figure 2. The relative fluorescence change of 0.1 μM (A) A10-2AP, (B) G10-2AP, (C) T10-2AP and (D) C10-2AP DNA after adding 2 μM various metal ions.

3.4. Hg^{2+} detection using T10-2AP DNA. With these probes, we might detect Hg^{2+} and Ag^+. We next aim to test the sensitivity for their detection. The above studies indicate that T10-2AP is

the best probe for Hg^{2+}. A scheme of the T-Hg^{2+}-T complex is drawn in Figure 3A, and the detection scheme is presented in Figure 3B, where folding of the DNA relaxes the 2AP base stacking and enhances its fluorescence.

The fluorescence gradually increased at higher Hg^{2+} concentrations (Figure 3C). We further plotted the peak intensity at 370 nm against Hg^{2+} concentration (Figure 3D). A sigmoidal binding curve was obtained, suggesting metal binding cooperatively. The signaling kinetics were measured with 400 nM Hg^{2+} (inset of Figure 3E). Although the majority of signal increase occurred in the first 30 sec (the time we used for collecting the data in Figure 3D), there is a slower phase taking a few minutes to finish.

Next, we also tested the effect of DNA length using a longer DNA containing 11 potential T-Hg^{2+}-T pairing bases (named T22-2AP, Figure S1). However, this longer probe is about 10 times less sensitive than the T10-2AP, possibly due to misfolding and the requirement of more Hg^{2+} to fold. We did not try even shorter DNA since five base pairs are typically required to form a stable hairpin. Therefore, our current probe is optimal for Hg^{2+} sensing.

With the T10-2AP probe, a roughly linear response was observed with up to 400 nM Hg^{2+} (Figure 4D, inset). Based on the 3σ/slope calculation (σ = background variation in the absence of Hg^{2+}), the detection limit is 3 nM Hg^{2+}, below the maximum level of mercury (10 nM) permitted by the U.S. Environmental Protection Agency (U.S. EPA) for drinking water. With 800 nM Hg^{2+}, the fluorescence enhancement reached nearly 14-fold (Figure 3D), indicating a high sensitivity. Such strong 2AP fluorescence enhancement was only observed in nuclease assays, where the 2AP was completely released from the DNA after enzymatic digestion (Su et al. 2012; Zhang et al. 2014). Some other enzymes, such as the EcoRI DNA methyltransferase,

can disrupt base stacking and even flip DNA bases; they can also achieve a significant fluorescence increase (Allan and Reich 1996). Therefore, we suspect that the 2AP base here might also flip from being base stacked to solvent exposed after Hg^{2+} binding. In most other systems, the enhancement was much less. The closet aptamer system achieved 5-10 fold enhancement for protein detection (Katilius et al. 2006). Detection of small molecules using 2AP has not achieved such high sensitivity. For example, even with engineered basic sites, only a signal-off sensor was reported for theophylline detection (Li et al. 2009a). While a signal-on aptasensor was reported using the structure-switching design, the fluorescence increase was less than 2-fold (Li and Ho 2008).

We further studied sensor specificity against various metal ions at (0.2 μM and 2 μM, Figure 3E). Among the tested metal ions, only Hg^{2+} showed an obvious fluorescence increase at both concentrations, further confirming a high selectivity towards Hg^{2+}. We noticed that with 2 μM Hg^{2+}, the fluorescence enhancement was only ~7-fold, less than the 14-fold achieved with 0.8 μM Hg^{2+} (Figure 3D, E), which is explained by that high concentrations of Hg^{2+} can non-specifically quench the 2AP fluorescence (Figure 1E).

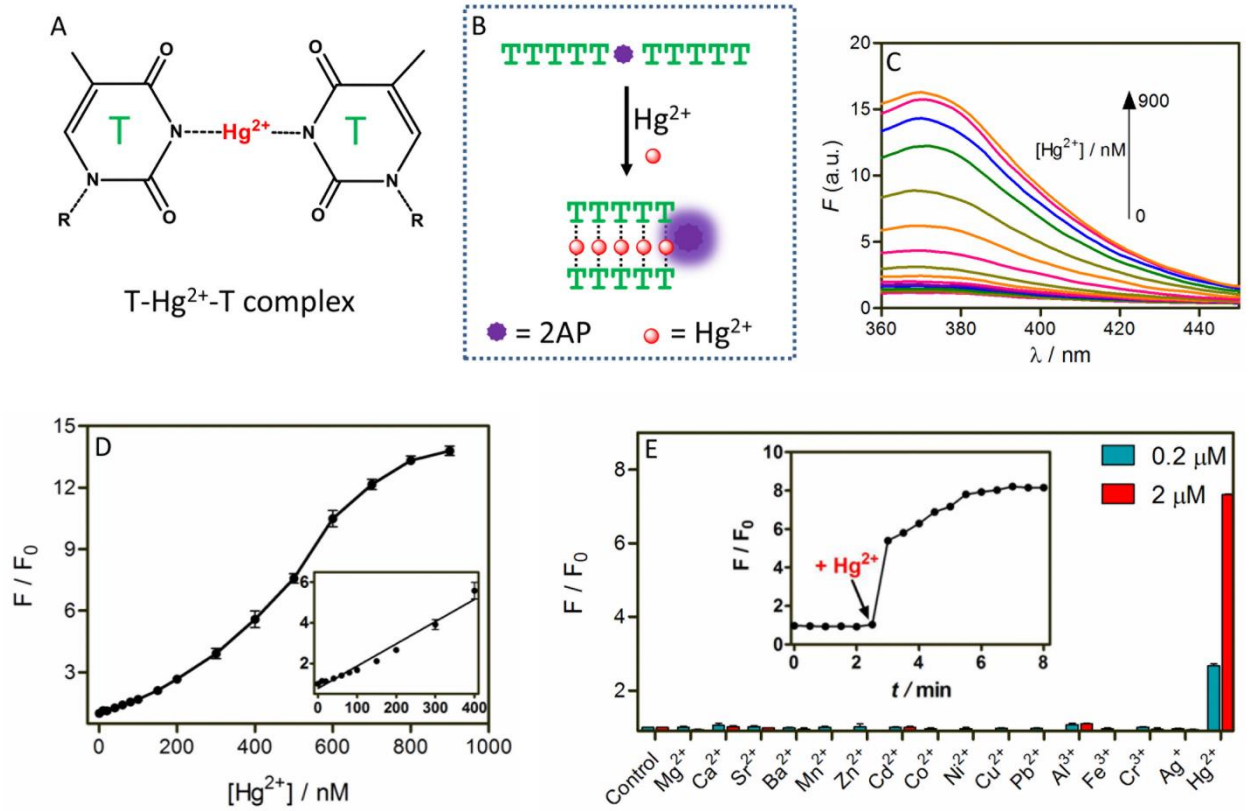

Figure 3. (A) The structure of a T-Hg^{2+}-T complex. (B) A scheme showing the fluorescence increase of the T10-2AP DNA by Hg^{2+}. (C) The fluorescence spectra of the Hg^{2+} sensor with increasing Hg^{2+} concentrations. (D) Sensor response as a function of Hg^{2+} concentration. Inset: linear fluorescence enhancement at low Hg^{2+} concentrations. (E) Sensor specificity tested with 0.2 and 2 μM various metal ions. Inset: the signaling kinetics of the sensor with 400 nM Hg^{2+}.

3.5. Highly robust Hg^{2+} sensing. To test the effect of buffer conditions, we next measured the sensor response at different pH values. The sensitivity is higher for Hg^{2+} at higher pH (Figure S2A). On the other hand, the fluorescence intensity of free 2AP and T10-2AP are insensitive to pH in the absence of Hg^{2+}. Therefore, the Hg^{2+} sensor works better at higher pH (Figure S2B),

which is attributable to the required deprotonation of N3 in thymine facilitating T-Hg^{2+}-T mismatch formation (Miyake et al. 2006).

For sensing in real water samples, one can easily adjust the pH by using a buffer, but it is more difficult to control or even measure the ionic strength. Since DNA is a polyanion that can be easily condensed at high salt concentrations, ionic strength usually severely affects DNA-based sensors. By reading the literature, while the T-Hg^{2+}-T binding mechanism has been extensively employed, few have addressed the ionic strength issue (Huang et al. 2016; Kiy et al. 2012). One popular signaling method is to label a fluorophore and a quencher respectively on the two ends of a thymine-rich DNA, so that Hg^{2+} binding can shorten the end-to-end distance and thus induce fluorescence quenching (Ono and Togashi 2004). We previously carefully studied the conformation of such DNA as a function of ionic strength, and observed non-specific DNA folding by salt, causing false positive signals (Kiy et al. 2012).

Herein, we measured our T10-2AP sensor response to 400 nM Hg^{2+} at different $NaNO_3$ concentrations (Figure 4A). The best sensitivity was achieved with 60 mM Na^+, and the variation was quite small (coefficient of variation ~10%). An important feature of this sensor design is that it contains only a single molecule and a single label. Its signaling depends mainly on the local base stacking environment of the 2AP base instead of DNA global folding. This can explain its robustness.

To have a full comparison, we also tested two more signaling strategies. First, a FAM-labeled DNA was adsorbed on graphene oxide (GO), resulting in quenched initial fluorescence. Hg^{2+} can induce DNA desorption and thus fluorescence enhancement (Figure 4B) (Lu et al. 2016). In the second example, SYBR Green I (SG) was used to stain the DNA hairpin formed

after adding Hg^{2+}, which also significantly enhances the emission intensity (Figure 4C). Without Hg^{2+}, the DNA has a random coiled structure and cannot enhance the SG emission. This is a cost-effective label-free method (Wang and Liu 2008). In both examples, we measured the signal in 0 and 100 mM $NaNO_3$ (Figure 4D). The GO signaling enhanced from less than 3-fold in the absence of salt to over 10-fold with 100 mM $NaNO_3$, which is likely due to the adsorption between DNA and GO is affected by salt (Wu et al. 2011). On the other hand, $NaNO_3$ strongly decreased the SG fluorescence attributable to a charge screening effect weakening DNA/SG interaction (Zipper et al. 2004), which affected both the initial background and the final signal after Hg^{2+} addition. Since the background fluorescence was affected more, the signaling also increased with 100 mM $NaNO_3$. The robustness of the 2AP label is attributable its signaling being less dependent of DNA hybridization (or duplex formation), end-to-end distance change, or electrostatic interactions, while most other sensing strategies rely on these.

All these methods have an excellent sensitivity. Using SG, Hg^{2+} can be detected down to 1.3 nM (Wang and Liu 2008), which is better than that of the GO-based method (LOD = 20 nM) (Lu et al. 2016). Our 2AP sensor also achieved a detection limit of 3 nM. The main advantage of our sensor is its robustness. In addition, our detection process is much simpler, requiring just a simple mixing step, while other methods need to either pre-adsorb DNA probes on GO or further adding SG.

3.6. Sensor regeneration. For practical applications, sensors need to have a reversible responses to allow for continuous monitoring of the analyte concentration fluctuation. To test this, we employed iodide to modulate Hg^{2+} concentration. Iodide binds Hg^{2+} with extremely high affinity and it can reduce the free Hg^{2+} in solution. We started by adding 400 nM Hg^{2+} to the sensor, and a significant fluorescence increase was observed immediately. Five minutes later, 800 nM I^- was

added and the signal dropped back to the background level (Figure 4E). Further adding Hg^{2+} enhanced the fluorescence again, which demonstrated sensor reversibility. After a few cycles, the maximal fluorescence decreased progressively. This could be due to the accumulation of HgI_2, which may non-specifically adsorb the DNA and quench the fluorescence.

3.7. Sensing in lake water. To test the sensor performance in real water samples, we collected water from Lake Huron. The final test solution consisted of 99% lake water and 1% the sensor containing buffer. When titrated this solution with different Hg^{2+} concentrations, a fluorescence increase similar to that in the pure water was observed (Figure 4F). The sensor can detect Hg^{2+} in the lake water up to 600 nM, with a detection limit of 8.4 nM Hg^{2+}. Therefore, this sensor is useful for detecting Hg^{2+} in environmental water samples.

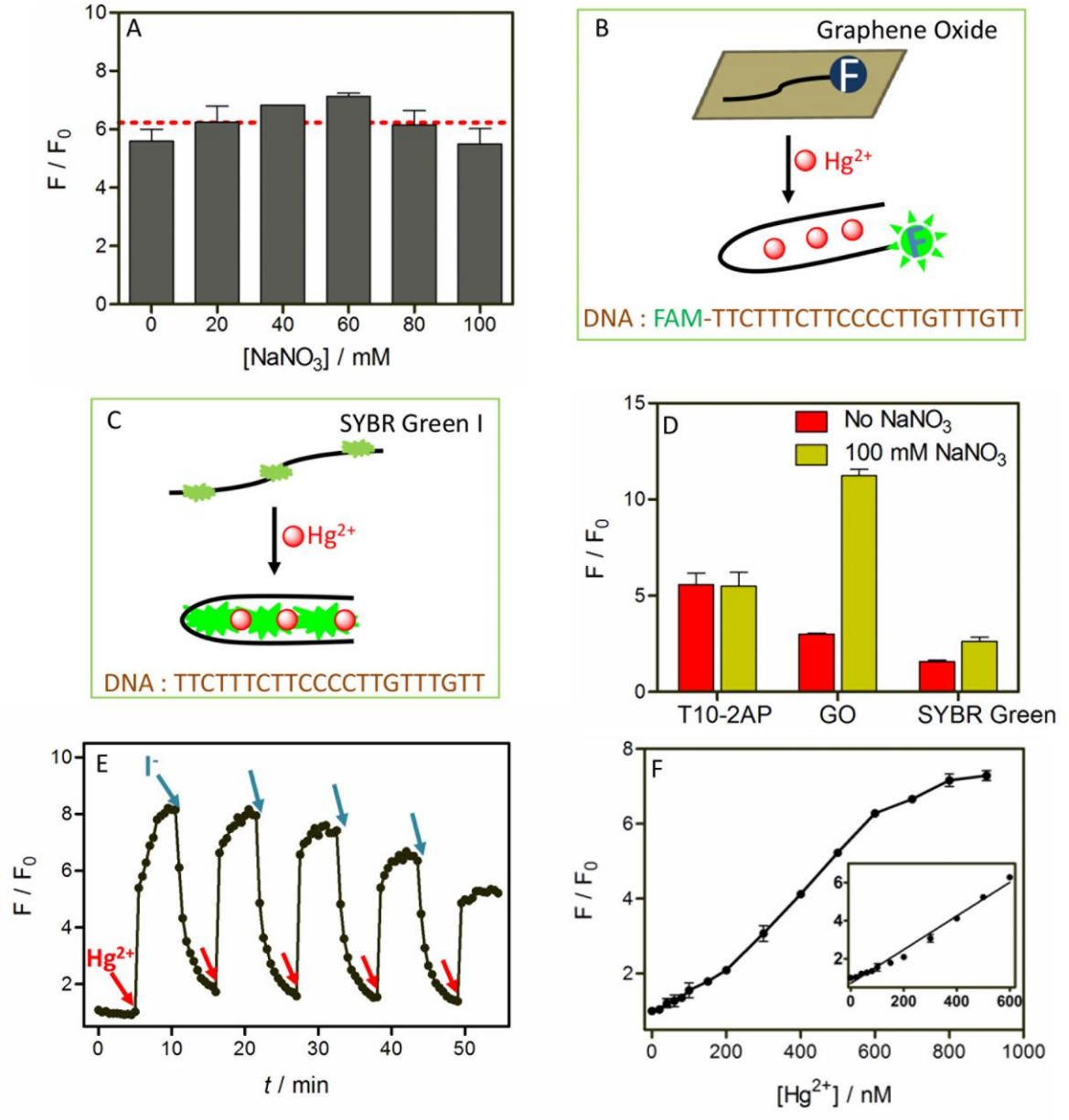

Figure 4. (A) The T10-2AP DNA sensor response with 400 nM Hg^{2+} under different $NaNO_3$ concentrations. Schemes illustrating (B) GO-based and (C) SG-based sensors for Hg^{2+} detection. (D) Comparison the signaling of each sensor with 400 nM Hg^{2+} in the absence and presence of 100 mM $NaNO_3$. (E) The T10-2AP sensor reversibility test. Hg^{2+} and I^- were added at 400 nM and 800 nM each time, respectively. (F) The sensor response as a function of Hg^{2+} concentration

in 99% of Lake Huron water. Inset: the fluorescence linearly increases at low Hg^{2+} concentrations.

3.8. Ag^+ detection using C10-2AP. Having demonstrated the use of T10-2AP for Hg^{2+} detection, we next explored the C10-2AP DNA for Ag^+ detection. The structure C-Ag^+-C is shown in Figure 5A, and the scheme of sensing is presented in Figure 5B, which is quite similar to that for Hg^{2+} detection described above. To test the sensor, we first measured the sensor fluorescence spectra before and after adding 700 nM Ag^+, where a significant fluorescence increase was achieved (Figure 5C). A more careful titration showed that the fluorescence of the sensor increases gradually with increasing Ag^+ concentration (Figure 5D). The fluorescence reached a plateau with ~500 nM Ag^+, and this is consistent with each DNA binding five Ag^+ ions (100 nM DNA used). Under the same condition, the T10-2AP DNA needs ~8 Hg^{2+} to achieve saturated binding (Figure 3D). In this aspect, the C-Ag^+-C complex appears slightly more stable than the T-Hg^{2+}-T complex. In the range of 0-400 nM Ag^+, the sensor has a linear response (inset of Figure 5D) with a detection limit of 3 nM Ag^+, significantly lower than the toxic level described by the U.S. EPA for drinking water (460 nM). Finally, we tested the sensor specificity with 2 and 0.2 μM various metal ions (Figure 5E). It is interesting to note that the signal from Hg^{2+} was significantly lower at 0.2 μM metal concentration (only about 20% of the Ag^+ signal), while at 2 μM, it is over half of the Ag^+ signal. This is consistent with the selective binding of Ag^+ by cytosine (Ono et al. 2008; Ono et al. 2011). At much higher metal concentrations, however, Hg^{2+} can still show significant binding.

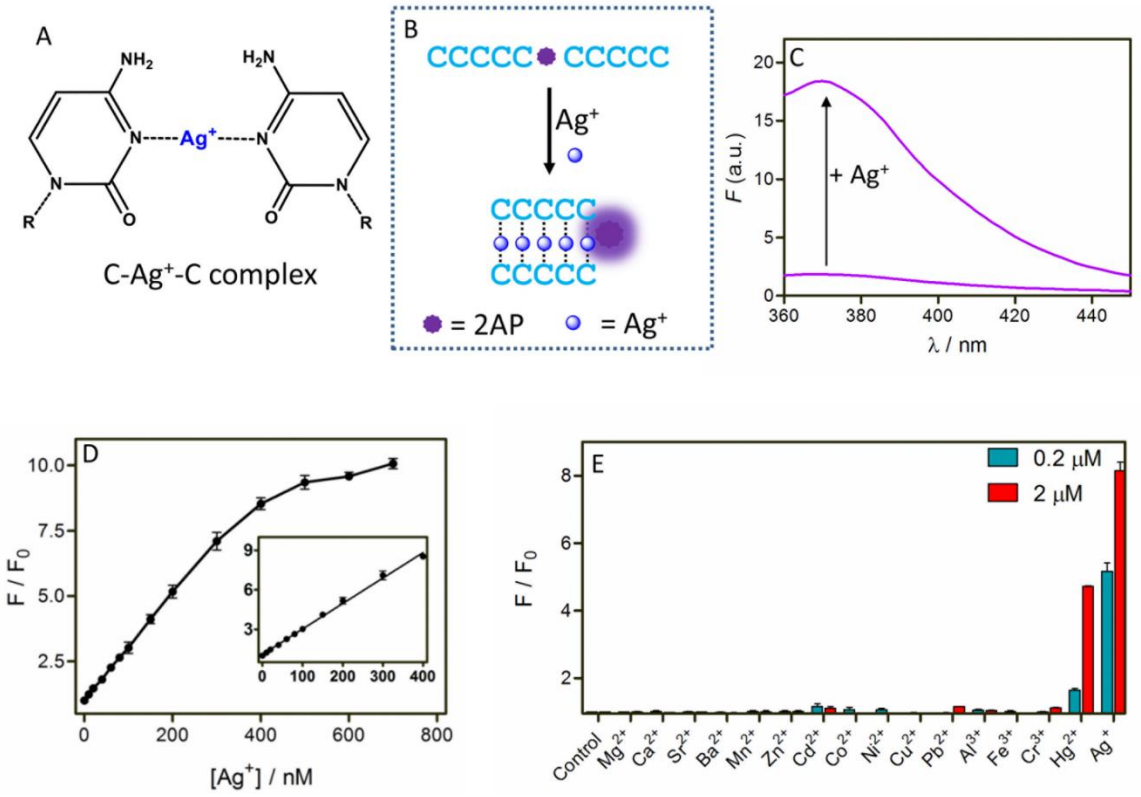

Figure 5. (A) The structure of C-Ag^+-C complex. (B) A scheme showing the fluorescence increase of the C10-2AP DNA caused by Ag^+. (C) The fluorescence spectra of this sensor in absence and presence of 700 nM Ag^+. (D) Sensor response as a function of Ag^+ concentration. Inset: sensor linear response at low Ag^+ concentrations. (E) Sensor specificity with 0.2 and 2 μM of various metal ions.

4. Conclusions.

In summary, we reported the first heavy metal sensors using 2AP signaling. This comprehensive study has included all the four DNA homopolymers and most common metal ions. With this

simple sensor design, we showed that 2AP is a highly robust fluorescent label in DNA. The advantage of 2AP is its sensitivity to the local base stacking environment and insensitivity to non-specific DNA condensation. Therefore, it can solve the ionic strength dependent problem for DNA-based sensors. W compared the 2AP-based sensors with three other signaling strategies using the same Hg^{2+} recognition chemistry. Taken together, this work has provided robust sensors for Hg^{2+} and Ag^{+}, and the same design method is likely applicable to other analytes.

Acknowledgement

This work is supported by the University of Waterloo, the Natural Sciences and Engineering Research Council of Canada (NSERC), Foundation for Shenghua Scholar of Central South University and the National Natural Science Foundation of China (Grant No. 21301195). W.Z. is supported by the Fellowship from the China Scholarship Council (CSC, Grant No. 201406370116).

Supporting Information Available: The following files are available free of charge.

Effect of DNA length and pH value on sensor performance.

References

1. Allan, B.W., Reich, N.O., 1996. Biochemistry 35, 14757-14762.
2. Clarkson, T.W., Magos, L., Myers, G.J., 2003. N. Engl. J. Med. 349, 1731-1737.

3. Hall, K.B., 2009. Chapter 13 - 2-Aminopurine as a Probe of RNA Conformational Transitions. Meth. Enzymol., pp. 269-285. Academic Press.
4. Hollenstein, M., Hipolito, C., Lam, C., Dietrich, D., Perrin, D.M., 2008. Angew. Chem., Int. Ed. 47, 4346 - 4350.
5. Huang, P.-J.J., Liu, J., 2014. Anal. Chem. 86, 5999-6005.
6. Huang, P.-J.J., van Ballegooie, C., Liu, J., 2016. Analyst 141, 3788-3793.
7. Huang, P.-J.J., Wang, F., Liu, J., 2015. Anal. Chem. 87, 6890–6895.
8. Jones, A.C., Neely, R.K., 2015. Quarterly Reviews of Biophysics 48, 244-279.
9. Katilius, E., Katiliene, Z., Woodbury, N.W., 2006. Anal. Chem. 78, 6484-6489.
10. Kelley, S.O., Barton, J.K., 1999. Science 283, 375-381.
11. Kim, H.N., Ren, W.X., Kim, J.S., Yoon, J., 2012. Chem. Soc. Rev. 41, 3210-3244.
12. Kiy, M.M., Jacobi, Z.E., Liu, J., 2012. Chem. Eur. J 18, 1202-1208.
13. Larsen, O.F.A., van Stokkum, I.H.M., de Weerd, F.L., Vengris, M., Aravindakumar, C.T., van Grondelle, R., Geacintov, N.E., van Amerongen, H., 2004. Phys. Chem. Chem. Phys. 6, 154-160.
14. Lee, J., Park, J., Hee Lee, H., Park, H., Kim, H.I., Kim, W.J., 2015. Biosens. Bioelectron. 68, 642-647.
15. Li, D., Song, S.P., Fan, C.H., 2010. Acc. Chem. Res. 43, 631-641.
16. Li, D., Wieckowska, A., Willner, I., 2008. Angew. Chem. Int. Ed. 47, 3927-3931.
17. Li, M., Sato, Y., Nishizawa, S., Seino, T., Nakamura, K., Teramae, N., 2009a. J. Am. Chem. Soc. 131, 2448-2449.
18. Li, N., Ho, C.-M., 2008. J. Am. Chem. Soc. 130, 2380-2381.
19. Li, T., Shi, L., Wang, E., Dong, S., 2009b. Chem. Eur. J 15, 3347-3350.

20. Lin, Y.-H., Tseng, W.-L., 2009. Chem. Commun., 6619-6621.

21. Liu, J., Cao, Z., Lu, Y., 2009. Chem. Rev. 109, 1948–1998.

22. Lu, C., Jimmy Huang, P.-J., Ying, Y., Liu, J., 2016. Biosens. Bioelectron. 79, 244-250.

23. Martí, A.A., Jockusch, S., Li, Z., Ju, J., Turro, N.J., 2006. Nucleic Acids Res. 34, e50.

24. Miyake, Y., Togashi, H., Tashiro, M., Yamaguchi, H., Oda, S., Kudo, M., Tanaka, Y., Kondo, Y., Sawa, R., Fujimoto, T., Machinami, T., Ono, A., 2006. J. Am. Chem. Soc. 128, 2172.

25. Morishita, K., MacLean, J.L., Liu, B., Jiang, H., Liu, J., 2013. Nanoscale 5, 2840-2849.

26. Nazarenko, I., Pires, R., Lowe, B., Obaidy, M., Rashtchian, A., 2002. Nucleic Acids Res. 30, 2089-2195.

27. Nolan, E.M., Lippard, S.J., 2008. Chem. Rev. 108, 3443-3480.

28. Nutiu, R., Li, Y., 2003. J. Am. Chem. Soc. 125, 4771-4778.

29. Ono, A., Cao, S., Togashi, H., Tashiro, M., Fujimoto, T., Machinami, T., Oda, S., Miyake, Y., Okamoto, I., Tanaka, Y., 2008. Chem. Commun., 4825-4827.

30. Ono, A., Togashi, H., 2004. Angew. Chem., Int. Ed. 43, 4300-4302.

31. Ono, A., Torigoe, H., Tanaka, Y., Okamoto, I., 2011. Chem. Soc. Rev. 40, 5855-5866.

32. Rachofsky, E.L., Seibert, E., Stivers, J.T., Osman, R., Ross, J.B.A., 2001. Biochemistry 40, 957-967.

33. Ratte, H.T., 1999. Environ. Toxicol. Chem. 18, 89-108.

34. Saran, R., Liu, J., 2016. Anal. Chem. 88, 4014–4020.

35. Shiang, Y.-C., Huang, C.-C., Chen, W.-Y., Chen, P.-C., Chang, H.-T., 2012. J. Mater. Chem. 22, 12972-12982.

36. Soulière, M.F., Haller, A., Rieder, R., Micura, R., 2011. J. Am. Chem. Soc. 133, 16161-16167.

37. Su, X., Zhu, X., Zhang, C., Xiao, X., Zhao, M., 2012. Anal. Chem. 84, 5059-5065.

38. Tanaka, Y., Oda, S., Yamaguchi, H., Kondo, Y., Kojima, C., Ono, A., 2007. J. Am. Chem. Soc. 129, 244.

39. Tyagi, S., Kramer, F.R., 1996. Nat. Biotechnol. 14, 303-308.

40. Urata, H., Yamaguchi, E., Nakamura, Y., Wada, S.-i., 2011. Chem. Commun. 47, 941-943.

41. Wang, H., Yang, R.H., Yang, L., Tan, W.H., 2009a. ACS Nano 3, 2451-2460.

42. Wang, J., Liu, B., 2008. Chem. Commun., 4759-4761.

43. Wang, K.M., Tang, Z.W., Yang, C.Y.J., Kim, Y.M., Fang, X.H., Li, W., Wu, Y.R., Medley, C.D., Cao, Z.H., Li, J., Colon, P., Lin, H., Tan, W.H., 2009b. Angew. Chem. Int. Ed. 48, 856-870.

44. Wang, Z., Lee, J.H., Lu, Y., 2008. Chem. Commun., 6005-6007.

45. Wu, M., Kempaiah, R., Huang, P.-J.J., Maheshwari, V., Liu, J., 2011. Langmuir 27, 2731–2738.

46. Zhan, S., Wu, Y., Wang, L., Zhan, X., Zhou, P., 2016. Biosens. Bioelectron. 86, 353-368.

47. Zhang, P., Zhang, J., Wang, C., Liu, C., Wang, H., Li, Z., 2014. Anal. Chem. 86, 1076-1082.

48. Zhang, X.-B., Kong, R.-M., Lu, Y., 2011. Annu. Rev. Anal. Chem. 4, 105-128.

49. Zhou, Y., Tian, X.-L., Li, Y.-S., Zhang, Y.-Y., Yang, L., Zhang, J.-H., Wang, X.-R., Lu, S.-Y., Ren, H.-L., Liu, Z.-S., 2011. Biosens. Bioelectron. 30, 310-314.

50. Zipper, H., Brunner, H., Bernhagen, J., Vitzthum, F., 2004. Nucleic Acids Res. 32, e103.